Chall. Nano Micro Scale Sci. Tech., 9(2):126-134, Summer and Autumn 2021
DOI: 10.22111/CNMST.2022.40773.1220

ORIGINAL RESEARCH PAPER

Effect of Geometric Parameters on the performance of Dry Gas Seal with Trapezoidal Grooves

Naghmeh Jamshidi[1*], Mohammad Rasoul Ebrahimi[2]

[1]Assistant professor, Department of Mechanical Engineering, Payame Noor University (PNU), Tehran, Iran.
[2]Department of Mechanical Engineering, Payame Noor University (PNU), Tehran, Iran.

Received 28 November 2021; revised 22 January 2022; accepted 17 February 2022;

ABSTRACT: Friction is created in the gas seals due to the relative motion of the two fixed and rotary surfaces, causing power dissipation, erosion, heat generation and temperature rise of the surfaces so a distance between two surfaces should be created. In the structure of Dry Gas Seals (DGS), the grooves on the rotating surface are created, which is the key to the gas penetration between the surfaces. The geometrical parameters of grooves would have substantial effect on the amount of leakage, so it is of high importance to indicate the best shape and operating condition of grooves. In this research, the effect of geometric parameters of a DGS with trapezoidal grooves on the leakage rate and open force is investigated. The geometric parameters are the depth of the triangular and square sections, the length of the groove, the angle of the square part and the angle of the groove. The length of the groove has a substantial impact on leakage, and by doubling the length, the leakage rate is raised to 58%. It is concluded that when the angle of the square section is 7° and the angle of groove is 22°, the minimum leakage occurs in the range of parameters studied. Taguchi algorithm is also applied to optimize the shape parameters of the groove to minimize open force and leakage of the seal. Optimal dimensions for grooves in the range of operating conditions in this study are $\text{triangle depth} = 3\mu\text{m}, \text{quad} - \text{depth} = 10\mu\text{m}, \text{Length} = 8\text{mm}, \text{groove angle} = 18°, \text{rectangle angle} = 5°$. The same optimum conditions are obtained by considering energy and exergy terms.

KEYWORDS: *DGS, Computational fluid dynamics, Open force, Leakage*

INTRODUCTION

A dry gas seal (DGS) is a typical mechanical device that is installed on the shaft to prevent gas leakage from the space between the shaft and the compressor shell, which can be caused by high-pressure gas behind this space. Since this piece is used to prevent leakage between a fixed and a rotating device, it is a kind of dynamic seal. Pressure-Driven Gas Flows were studied in the literature [1, 2] . In DGS by directing the gas into space between two fixed and rotating surfaces, there is a slight distance between surfaces, and by removing the sliding motion between the plates, the friction is significantly reduced. On the other hand, by passing gas through the two surfaces into the atmosphere, the heat generated by the shear stress is also transmitted, and the possibility of permanent use of the seal is provided. Therefore, in the design of DGS, the gas leak is predicted in advance to a certain extent. The entrance region exhibited a maximum increase in heat transfer, which decreases with an increase in the distance from the inlet. When x/D increased from 63 to 173 at Re=1600, it decreased from 47% to 14%. A closer look at the structure of the DGS indicates that on the rotating surfaces, grooves are created, which are the key to penetrating the gas between two fixed and rotating surfaces. Types of grooves can be spiral, T-shaped, trapezoidal grooves, etc.

*Corresponding Author Email: *n.jamshidi@pnu.ac.ir*
Tel.: +989198506567; Note. This manuscript was submitted on November 28, 2021; approved on January 22.

Researchers have been studied DGSs with different types of groove shapes such as Shahin et al. [3] and Ma et al. [4] who have studied spiral type grooves or another work by Ma et al. [5] that examined T-shaped grooves. As far as the scale of grooves is microscopic, in some cases, the micro effect should be studied, so Wang et al. [6] considered micro effects in a spiral groove. Shahin et al. [3] conducted a three-dimensional computational study on DGSs with conical spiral type grooves. Their simulation consisted of two sections, fixed and narrowing groove depth. Their investigation shows that when the thickness of the thin film is increased, the open force decreases so the amount of gas leakage increases. Huiqiang [7] performed numerical analyzes in DGS with helical grooves in micro scales. The gas film and also the grooves are only a few microns so that in some circumstances micro-scale effects are noticeable and can significantly affect the performance of DGS. Numerical results show that the average pressure in the gas film and the leakage of seal increases due to micro-scale effects and as a result, the open force increases. At low compression pressures and low-speed rotation, frictional torque and power consumption remain constant. The study by Su et al.[8] used solving 3D Navier-Stokes momentum and continuity equations in different grooved gas seals.

Nomenclature

A	x-y cross section side of grove, (mm^2)	T	Temperature, (K)
c_p	specific heat capacity, (J/kg. ℃)	T_0	inlet flow temperature, (K)
d	Intermediate groove width, (μm)	V	velocity field, (m/s)
F	Opening force, (N)		**Greek Letters**
h	Specific enthalpy, (J/kg)	α_1	The spiral angle in the top of groove, (°)
k	thermal conductivity coefficient, (W/m. K)	α_2	The spiral angle at the bottom of groove, (°)
K_n	Knudson Number$(\frac{\mu\sqrt{2RT_0}}{Ph})$	ρ	Gas density , (kg/m^3)
L	Leakage, $(\frac{cc}{s})$	μ	dynamic viscosity of the gas, $(\frac{kg}{ms})$
$\dot{m}$	Mass flow rate, $(\frac{kg}{s})$	φ	Angle of grooved surface, (°)
n	Number of grooves	Φ	heat source
P	Pressure, (Pa)	θ	Angle of an annular sector, (°)
r_i	Inner radius of seal, (μm)		**subscripts**
r_o	Outer radius of seal, (μm)	In	inlet
r_{g1}	Lower groove radius, (μm)	Out	Outlet
r_{g2}	Upper groove radius, (μm)	L	Left hand side
Re	Reynolds number $(\frac{\rho V\delta}{\mu})$	R	Right hand side

Du et al. [9] used the real gas model to evaluate the sealing performance of grooved ring in rotation. The stated that rotation has a significant effect on the sealing performance.

Yan et al. [10] examined the effect of roughness on groove bottom can boot the sealing performance of the dry gas seal. The depth, width and pitch of the opening force and leaking rate but the optimal condition should be assessed in the study. The effect of turbulence fluid flow characteristics was studied both experimentally and numerically by Yan et al. [11] . In low rotational speed and pressure condition, the fluid flow is laminar; however, with the increase in rotational speed the flow regime moves toward being turbulence. They concluded that the adiabatic boundary condition is closer to the real flow, in comparison to isothermal boundary condition. An analytical model was developed by Zahorulko et al. [12] on the effect of a direct action gas difference pressure regulator in dry gas seals for obtaining the required pressure difference of a compressor. They concluded that in both static and dynamic mode, an appropriate selection of damping chamber geometry can damp the vibration significantly.

Taguchi method can be applied to find the best condition according to the operating conditions. This method consists of three design methods: system, parameter and tolerance methods. In the design of the parameter, the specified value of the parameters of the system is defined, and the design of the parameter gives the best value for the parameters in a system [13]. The goal of the design parameter is to obtain a state in which the character has the least-fluctuating return, and its value is close to its ideal value. Signal to Noise Ratio (SNR) is a measure of the rate of variation of efficiency affecting the selected parameters in the presence of noise factors. The primary goal is to bring the SNR value to its maximum. The orthogonal matrix plays an essential role in the Taguchi method and allows the examination of different design parameters through a quality attribute. Using the orthogonal matrix, we can obtain the effects of different factors simultaneously with a limited number of experiments. Regarding the number of design parameters and their level of variation in the range of study, a suitable orthogonal matrix can be chosen. In the literature, there are some studies performed by applying Taguchi method in heat transfer problems [14-19]. Bicer et al.[20] applied Taguchi model for three-zonal baffle to obtain higher rate of heat transfer and lower pressure loss, and by another work in this field Thondiyil and Kodakkattu [21] optimized the segregated baffles. Hashimoto and Ochiai [22] conducted a theoretical optimization and topological simulation on air driven bearings, which mainly have the stiffness of various air-lubricating films, and concluded that the optimization of the shape of the groove from the dry gas seals is utterly different from the spiral groove. The shape of the optimized groove is quite similar for different densities and internal pressure. Wang and Du [23] performed DGS structural optimization with a T-shaped groove. The results show that full use of the groove space efficiently reduces the wear of the dry gas seal surfaces, contributes to improving the work of the dry gas seals and its sealing effect, and this is done when the circumferential ratio is halved.

In this study, due to the importance of groove geometry on the fluid flow, a trapezoidal groove is selected, and the effect of geometric parameters such as the depth of the triangular and square trapezium section, the length, and angle of the grooves, on the leakage and the open force are investigated. Taguchi algorithm is applied, and the optimized shape is obtained after 27 different numerical simulations.

1. GOVERNING EQUATIONS AND SOLUTION METHOD

The Reynolds number indicates the allowable range for laminar flow. While Reynolds number remains below 4000 in this study, the conditions fall largely in the realm of laminar gas flow especially for low-speed operations with relatively small gaps.

Numerical simulations are performed using the ANSYS-Fluent Computational Fluid Dynamics software. The governing equations of fluid are as follows (9):

$$\frac{\partial}{\partial r}(\rho r V_r) + \frac{\partial}{\partial z}(\rho r V_z) = 0 \tag{1}$$

$$V_r \frac{\partial V_r}{\partial r} + V_z \frac{\partial V_z}{\partial z} - \frac{{V_\theta}^2}{r} = -\frac{1}{\rho}\frac{\partial P}{\partial r} + \frac{1}{\rho}\frac{\partial}{\partial z}\left(\mu \frac{\partial V_z}{\partial z}\right) \tag{2}$$

$$V_r \frac{\partial V_\theta}{\partial r} + V_z \frac{\partial V_\theta}{\partial z} + \frac{V_r V_\theta}{r} = \frac{1}{\rho}\frac{\partial}{\partial z}\left(\mu \frac{\partial V_\theta}{\partial z}\right) \tag{3}$$

$$\frac{1}{\rho}\frac{\partial P}{\partial z} = 0 \tag{4}$$

$$\frac{(\rho c_p T_g)}{\partial t} + \frac{\partial(\rho u_i c_p T_g)}{\partial x_i} = \frac{\partial}{\partial x_i}\left(k \frac{\partial T_g}{\partial x_i}\right) + q \tag{5}$$

In which T_g is gas temperature and q is heat source inside solid which mainly originates from the frictional losses in the contact.

Thermo-physical properties of the gas (air) are considered to be temperature dependent. The dynamic viscosity of the gas (μ), the thermal conductivity coefficient (k), the specific thermal conductivity (c_p), varies with temperature as equations (6-8)[8, 24].

$$\mu(T) = -8.38278 \times 10^{-7} + 8.35717 \times 10^{-8} T_g - 7.69430 \times 10^{-11} T_g^2 + 4.64373 \times 10^{-14} T_g^3 - 7.43864 \times 10^{-15} T_g^4 \tag{6}$$

$$k(T) = -2.27584 \times 10^{-3} + 1.15480 \times 10^{-4} T_g - 7.90253 \times 10^{-8} T_g^2 + 4.11702 \times 10^{-11} T_g^3 - 7.43864 \times 10^{-15} T_g^4 \tag{7}$$

$$c_p(\mathrm{T}) = +1.04764 \times 10^3 - 3.72589 \times 10^{-1} T_g + 9.45304 \times 10^{-4} T_g^2 - 6.02409 \times 10^{-7} T_g^3 + 1.28590 \times 10^{-10} T_g^4 \tag{8}$$

The SIMPLE algorithm is used for velocity and pressure coupling, and the second-order upwind method is used to discriminate the equations. The solution is converged when the residual of continuity, momentum and energy equations become less than 10^{-5}.

PHYSICAL MODEL AND GRID GENERATION

The seal includes a fixed surface (stator) and a rotating surface (rotor) and symmetrical trapezoidal grooves. Due to the symmetric distribution of the groove around the sealing surfaces, a sector consisting one single groove could be simulated. The DGS geometry is shown in Fig. 1. The complete geometry is shown in Fig. 1a, while the computational domain which is a 36° sector and the designated geometric parameters in this study are presented in Fig. 1b.

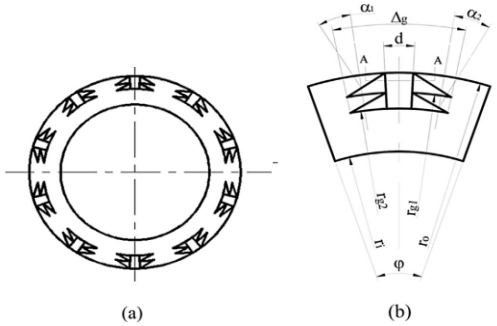

Fig. 1. a) The whole geometry of DGS with trapezoidal grooves, **b)** Computational domain in this study

Table 1
Dimensions of DGS

Characteristic	Dimensions
Outer radius (μm)	85230
Inner radius(μm)	60010
Number of slots	10
Rotor axial thickness(μm)	11080
Stator axial thickness(μm)	12650
Depth of trapezoid groove(μm)	5.27
Rectangular groove depth (μm)	18.5
Lower groove radius (μm)	73380
Upper groove radius(μm)	78920
The spiral angle in the top of groove (°)	27
The spiral angle at the bottom of groove(°)	27
Angle of grooved surface(°)	22.21
Intermediate groove width (μm)	8400

For convenient and controllable grid generation, computational domain is divided into ten regions and mesh generation is such that in the vicinity of the slots and the distance between the rotor and the stator, more intense meshes are created. By moving away from the groove and the rotor/stator, the grid density is reduced. The grid system is shown in Fig. 2.

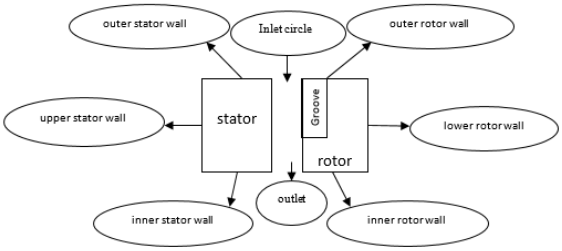

Fig. 1. applied boundary condition

The pressure on the inner and outer edges of the seal is considered to be constant. In addition, symmetry boundary conditions are assumed on the two lateral sides of the annular

section (Fig. 3). As a result, the pressure gradient at any radial position on the peripheral boundaries is zero. The continuity of the flow conditions determines that the amount of mass flow in and out of the contact plates in the peripheral direction must be equal, resulting in:

$$p(r_i, \theta, z) = p_{out}, \quad p(r_o, \theta, z) = p_{in} \tag{9}$$

$$T_{in} = 423^0 k, \ p_{out} = 0.1\ MPa, \ p_{in} = 4.5 MPa \tag{10}$$

$$\left(\frac{dp}{d\theta}\right)_{(r,\theta_L)} = \left(\frac{dp}{d\theta}\right)_{(r,\theta_R)} = 0 \tag{11}$$

$$\dot{m}(r, \theta_L) = \dot{m}(r, \theta_R) \tag{12}$$

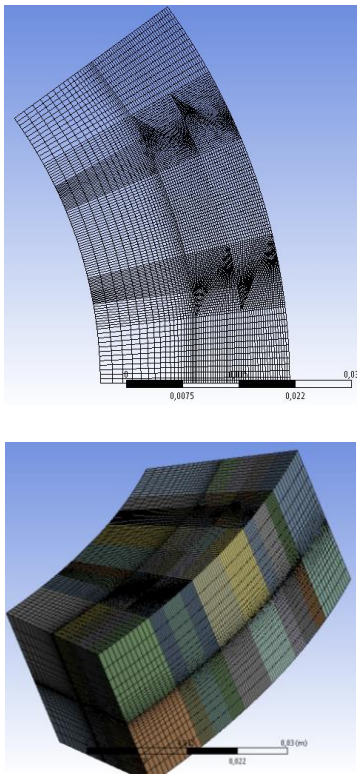

Fig. 3. Grid system used in the simulation

An adiabatic boundary condition is applied on stator inner and outer wall and rotor inner and outer wall, while convection heat transfer mechanism is available on the outer wall of stator and rotor. Inlet pressure is set to 4MPa and inlet temperature is set to 423K. The pressure inlet boundary condition is assumed for the inlet, the operating condition equal to 4 MPa or 4,000,000 Pa and the gage total pressure of 500,000 Pa to avoid divergency in the solution. To explain more, given that the value of the input speed is 5 m / s, the value of Initial gage pressure through the following equation, the value of which is 499347 psi. The inlet temperature is 423K.

$$P_{total} = P_{static} + \frac{\rho V^2}{2} \tag{13}$$

$$P_{total,abs} = P_{static,abs}\left(1 + \frac{k-1}{2} M^2\right)^{\frac{k}{k-1}} \tag{14}$$

$$T_{total,abs} = T_{static,abs}\left(1 + \frac{k-1}{2} M^2\right) \tag{15}$$

The outlet pressure boundary condition is used in the outlet. Because the operating pressure in the software is equal to 4,000,000 Pa, so in the case that the output pressure is equal to one atmosphere or 101,000 Pa the relative output pressure is equal to Pgage = -3899000. So, the gauge pressure value is set to 3899000.

The initialization is set on all boundaries. At first, the rotor speed equal to 11370 is not given to the software to avoid divergency, but the speed is set to zero and after 10 to 20 repetitions it is gradually increased to the desire speed over time. The rest of the solution remains convergent after 3230 repetitions. The problem is considered converged when the difference between the output and input boundary flows is less than 0.5% (0.055%) of the total flow rate.

1. TAGUCHI METHOD

In this study, the parameter design model of Taguchi method is applied. According to the Taguchi method, three types of quality characteristics "higher is the better"; "nominal is the best" and "lower is the better" may concern the target design. The purpose of this research is to determine the optimal values of various geometric parameters affecting the DGS groove force and leakage, so “the lower is the better” approach is applied. Design parameters are the depth of trapezoid groove, rectangular groove depth, groove length, groove angle and rectangle-angle; and the effect of these parameters on the open force and leakage are studied. Due to the dimensions of the groove under this study, the range of design parameters are as listed in Table 2 [25]; where five design parameters are divided into three levels.

Table 2
The range of design parameters

level	triangle-depth	quad-depth	length	groove-angle	rectangle-angle
	(μm)	(μm)	(mm)	($^\circ$)	($^\circ$)
1	3	10	8	18	5
2	6.5	17.5	12	22.5	7
3	10	25	16	27	9

Taguchi proposes an orthogonal array according to the number of design parameters and the level of each value's variation. The number of simulations is determined by the number of useful parameters and the level of changes of each variable using the orthogonal array. Using this matrix can ensure that each level of variables is repeated appropriately in all simulations. Various types of orthogonal arrays can be

used in Taguchi experiments. In this study Taguchi's analytical method is done using the Minitab 15.0 software, which is a computer program designed to perform advanced statistical operations. By applying Taguchi method in Minitab software, an orthogonal array with 27 simulations are proposed which are listed in Table 3.

Table 3
Simulations proposed by Taguchi

Run number	triangle-depth (μm)	quad-depth (μm)	length(mm)	groove-angle(°)	rectangle-angle(°)
1	3	10	8	18	5
2	3	10	8	18	7
3	3	10	8	18	9
4	3	17.5	12	22.5	5
5	3	17.5	12	22.5	7
6	3	17.5	12	22.5	9
7	3	25	16	27	5
8	3	25	16	27	7
9	3	25	16	27	9
10	6.5	10	8	27	5
11	6.5	10	8	27	7
12	6.5	10	8	27	9
13	6.5	17.5	12	18	5
14	6.5	17.5	12	18	7
15	6.5	17.5	12	18	9
16	6.5	25	16	22.5	5
17	6.5	25	16	22.5	7
18	6.5	25	16	22.5	9
19	10	10	8	22.5	5
20	10	10	8	22.5	7
21	10	10	8	22.5	9
22	10	17.5	12	27	5
23	10	17.5	12	27	7
24	10	17.5	12	27	9
25	10	25	16	18	5
26	10	25	16	18	7
27	10	25	16	18	9

By simulating these proposed experiments in the ANSYS FLUENT software, the open force and leakage for each case can be obtained. The results of simulations introduced by orthogonal array are then converted to SNR. In this study, the optimal values will be obtained by minimizing the open force and leakage. SNR conversion functions are defined according to the purpose of optimizing the characteristic of "less and better" performance as follows:

$$SNR = -10\ \log\left(\sum_{i=1}^{n} \frac{Y_i^2}{n}\right) \tag{19}$$

In these formulas, n is the number of repetitions in the $i-th$ simulation.

RESULTS AND DISCUSSIONS

Grid independence and verification

In this section, verification of grid system and solution procedure is done. Several different sizes of the computational grids are used to verify the suitability of the grid system, and the results are compared with the results of other researchers [24].

The results of the comparison of the three different grid system are shown in Table 4. In the case of the rotor and stator spacing of $3\mu m$, the grid and solution methods error in coarse, moderate and fine grids are 4%, 3.3%, and 3.1%, respectively. Due to the small difference between the results of moderate and fine grids systems, a system with 469064 elements is selected. By using the selected grid system at 7000rpm rotor speed, there would be 3.3% difference in the amount of gas leakage by present study and the study by Su et al. [24], which is acceptable.

Table 4
Grid independency and verification of solution procedure with Su et al.(24)

% error	Opening force(N)	Number of mesh elements
4%	42.33	198488
3.31%	42.05	469064
3.13%	41.98	780028

Investigating the effects of geometric parameters of dry gas seal

First, the effect of the depth of the triangular part of the seal on the open force and leakage is investigated. As shown in Fig. 4, By increasing the triangular depth, both open force, and leakage increase. The increase of open force by changing the depth from $3-10\ \mu m$ is about 2% while it is about 17.5% for leakage.

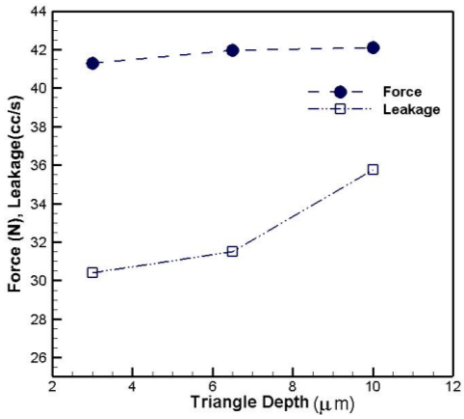

Fig. 4. The effect of the depth of the triangular part of the seal on the open and leakage forces

Figure 5 shows the velocity flow field contours, which in a similar way show the trend of changes in the pressure field. This figure shows that the velocity of the gas in the grooved area is generally higher than the velocity of the gas on the non-grooved surface. In addition, the concentration of velocity, due to the sudden geometric discontinuity and sharp

edges, affects how the velocity is distributed at the edges of the triangular parts of the groove, and this concentration can be seen in the figure in red. This area could potentially be a place to generate quite turbulent flow. On the other hand, in the grooved area, near the inner edge of the seal, the flow velocity is somewhat improved due to its distance from the groove, and the velocity concentration is seen on the inner edge of the triangular groove, in other words, the velocity increases with the depth of the triangular groove. At the inner edge of the seal, the velocity values have also increased due to the velocity matching with the rotor surface.

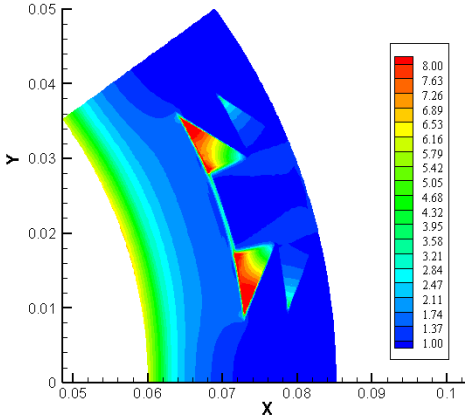

Fig. 5. The velocity contours in the cross section of seal in (m/s)

Investigating the effect of the depth of the square section of the groove on the force and leakage is shown in Fig. 6. Based on the diagram, it is deduced that the depth of the square of the groove on the open force is almost neglectable, however, increasing the depth from $10 - 25\ \mu m$, the leakage from the groove increases by 13.5%. The effect of depth changes in leakage is seen at higher depths. At the higher depth of quadrate part, the effect of depth on the leakage is more considerable.

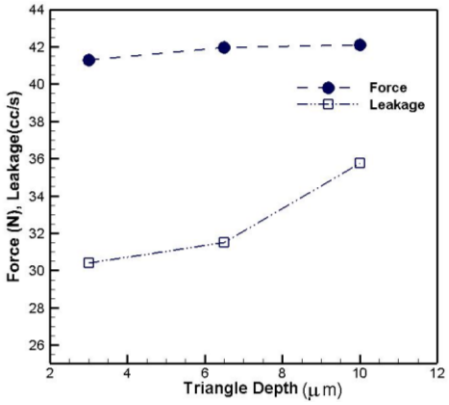

Fig. 6. Effects of Square depth of groove on open force and leakage

In Fig. 7, the effect of the groove length on the two-goal parameters in this study is shown. The effect of the length of the groove on the open and leakage force is considerable and doubling the length, the open force and leakage increase 12% and 58% respectively.

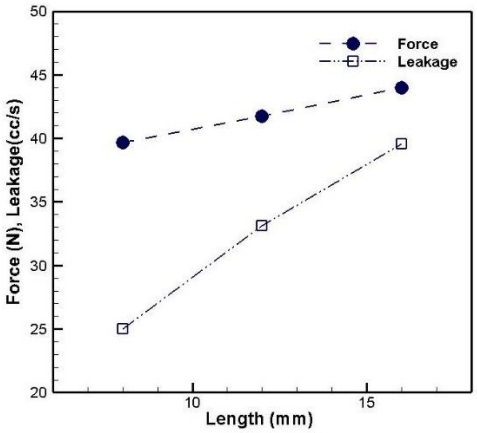

Fig. 7. Effect of the length of the groove on open force and leakage

Figures 8 and 9 show the effect of the groove angle and rectangle angle on the seal performance. Figure 8 shows the effect of the square section angle and Figure 9 shows the groove angle on the open force and leakage. As seen in the figure, in both cases there is an optimal amount of angle at which the leakage from the seal is minimized. These angles occur at the angle of the square and the angle of the groove about 7 and 22 º respectively.

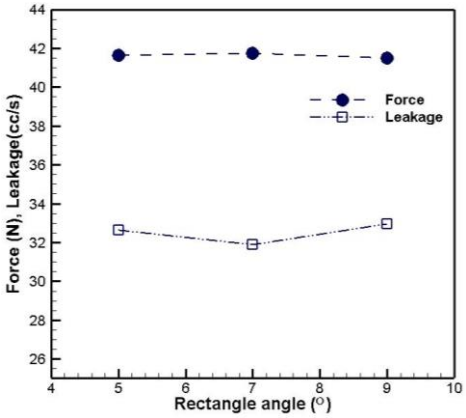

Fig. 8. Effect of squeegee angle on open and leakage forces

COMPUTATIONAL OPTIMIZATION

Minimizing the leakage and open force is one of the most significant challenges in designing a DGS. Taguchi method is used in this study to find the best geometry of trapezoidal groove. The procedure of finding optimum values has a number of simulations proposed in Table 3 and each simulation is conducted in ANSYS-FLUENT software. The computed leakage and open force for each simulation are listed in Table 5.

The outer and inner angles do not affect open force much, but the radial length of the groove or the longitudinal width

of the groove affects the open force, and to be optimal, the length of the groove should be minimized (Fig. 10).
The SNR for leakage reveals that the outer and inner angles do not have a significant effect on leakage, but the radial length of the groove or the longitudinal length of the groove have a substantial impact. The longitudinal groove should be 0.5 to have the optimum leakage. However, if the depth of the trapezoid groove and the rectangular groove are low, the amount of leakage will be less. From the review of the graphs, we conclude that the optimal conditions are as mentioned in Table 6.

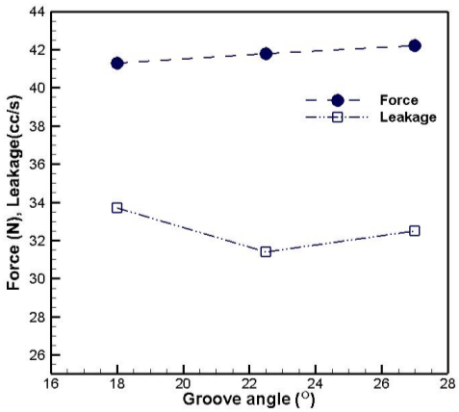

Fig. 9. Effect of the angle of the groove of the seal on open and leakage forces

Table 5
The amount of open force and leakage according to numerical simulation for each set of proposed experiment

No.	leakage	open force	No.	leakage	open force
1	21.458	38.499	15	39.63	43.851
2	22.913	38.751	16	25.258	39.613
3	22.674	39.299	17	25.328	39.714
4	28.391	40.99	18	25.408	39.803
5	28.899	41.209	19	38.887	44.266
6	28.932	41.477	20	39.015	44.365
7	41.43	43.783	21	41.15	44.5
8	37.801	43.754	22	27.772	40.2099
9	40.497	44.059	23	25.743	40.283
10	31.271	42.5195	24	27.929	40.377
11	30.0236	42.28	25	39.897	41.505
12	30.0168	42.43	26	39.959	41.557
13	39.2795	43.63	27	40.048	41.6
14	37.712	43.456			

In the case of energy and exergy analysis, the difference between input and output pressure, the difference between the output and input entropy (net entropy), and the difference between the input and output energy (net energy) are computed and listed in Table 7. The first row of Table 7 which is the optimum case considering open force and leakage, is the best case again. Optimal conditions are triangle depth= $3\mu m$, quad-depth= $10\mu m$, length= $8\,mm$, groove angle= $8°$, rectangle angle= $5°$.The lower output pressure results in the minimum leakage in one hand and minimum amount of pure energy and entropy on the other.

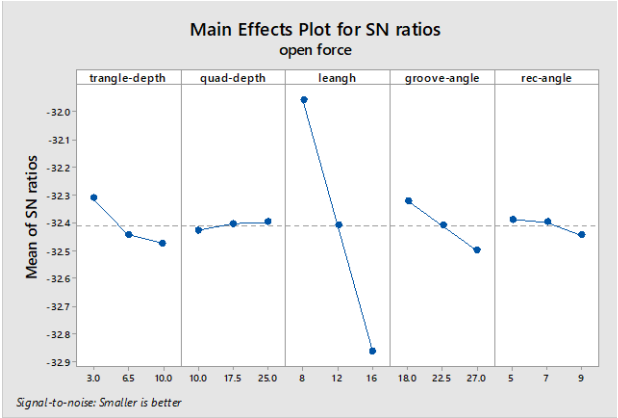

Fig. 10. SN values after inserting the simulation results into Taguchi algorithm.

Table 6
Optimal dimensions for grooves

Run number	triangle-depth (μm)	quad-depth (μm)	Length (mm)	groove-angle(°)	rectangle-angle(°)
1	3	10	8	18	5

CONCLUSION

In this paper, the effect of geometric parameters on the open force and leakage of a dry gas seal has been investigated numerically. The geometric parameters of the groove are the depth of the triangular and square sections of the groove, the length and angle of the groove, the square angle and the angle of the groove. Proper grid system and solving algorithm are applied to achieve the minimum deviations from references. Taguchi algorithm was applied to find the optimized shape parameters by objecting open force, and leakage. The following results are obtained:

- By increasing the depth of the square and triangular grooves, open force and leakage increase.
- The length of the groove is a critical factor for leakage of groove and by doubling the length of the groove, the leakage rate increases by 58%.
- The angle of the square section as 7° and the angle of the groove as 22° will minimize leakage from the seal.
- Optimal conditions in the range of current operating conditions are triangle depth= $3\mu m$, quad-depth= $10\mu m$, length= $8\,mm$, groove angle= $8°$, rectangle angle= $5°$.
- The optimized values are proved to be the best for the trapezoidal groove considering energy and entropy criteria.

Table 7
The values of pressure difference, net energy and net entropy for each case of study

Run number	Input and output pressure differences (Pa)	Net entropy value (kJ/K)	Net energy value(kJ)
1	2459800.4	425.81	1736.8
2	2521740.6	443.43	1740.2
3	2548557.1	450.7	1524.2
4	2553138.6	456.17	2776.1
5	2543695	452.77	2608.53
6	2536366.6	450.22	2498.8
7	2661766.8	495.28	4106.2
8	2505089.6	445.06	3733.3
9	2559184	461.05	3751.4
10	2599392	470.84	2951.1
11	2503432	440.15	2422.7
12	2498900	438.82	2420.55
13	2624402	481.51	3479.1
14	2530108.6	451.62	3240.44
15	2617066.5	477.27	2917.6
16	2581115.6	468.52	3975.67
17	2577566.8	467.26	3926.5
18	2575857.6	464.24	3162.41
19	2486367.1	438.23	3264.3
20	2482735.1	437.08	3225.9
21	2544815.5	454.57	3076.7
22	2634212.6	485.51	3970.63
23	2584666	470.55	4196.2
24	2629704.4	483.44	3798.5
25	2538272.9	458.98	5068
26	2536706	458.8	5154.1
27	2534854	456.6	4667.1

REFERENCES

[1] Aissa A, Slimani M-E-A, Mebarek-Oudina F, Fares R, Zaim A, Kolsi L, et al. Pressure-Driven Gas Flows in Micro Channels with a Slip Boundary: A Numerical Investigation. Fluid Dynamics \& Materials Processing. 2020; 16(2): 147-59.

[2] Gourari S, Mebarek-Oudina F, Makinde O, Rabhi M. Numerical Investigation of Gas-Liquid Two-Phase Flows in a Cylindrical Channel. Defect and Diffusion Forum. 2021; 409: 39-48.

[3] Shahin I, Gadala M, Alqaradawi M, Badr O. Three dimensional computational study for spiral dry gas seal with constant groove depth and different tapered grooves. Procedia Engineering. 2013; 68: 205-12.

[4] Ma G, Zhao W, Shen X. Analysis of Parameters and Performance for Spiral Grooved Cylindrical Gas Film Seal. Procedia Engineering. 2011; 23: 115-9.

[5] Ma C, Bai S, Peng X. Thermo-hydrodynamic characteristics of spiral groove gas face seals operating at low pressure. Tribology International. 2016; 95: 44-54.

[6] Wang B, Zhang H, Cao H. Flow dynamics of a spiral-groove dry-gas seal. Chinese Journal of Mechanical Engineering. 2013; 26(1): 78-84.

[7] Huiqiang WBZ. Numerical analysis of a spiral-groove dry-gas seal considering micro-scale effects. Chinese Journal of Mechanical Engineering. 2011; 24(1): 1.

[8] Su H, Rahmani R, Rahnejat H. Performance Evaluation of Bidirectional Dry Gas Seals with Special Groove Geometry. Tribology Transactions. 2017; 60(1): 58-69.

[9] Du Q, Gao K, Zhang D, Xie Y. Effects of grooved ring rotation and working fluid on the performance of dry gas seal. International Journal of Heat and Mass Transfer. 2018; 126: 1323-32.

[10] Yan W, Jianjun S, Qiong H, Da W, Xiaoqing Z. Orientation effect of orderly roughness microstructure on spiral groove dry gas seal. Tribology International. 2018; 126: 97-105.

[11] Yan R, Chen H, Zhang W, Hong X, Bao X, Ding X. Calculation and verification of flow field in supercritical carbon dioxide dry gas seal based on turbulent adiabatic flow model. Tribology International. 2022; 165: 107275.

[12] Zahorulko AV, Lee Y-B. Dynamic behavior and difference pressure control of difference pressure regulator for dry gas seals. Mechanical Systems and Signal Processing. 2022; 165: 108350.

[13] Rajabi Aref AJ, Fallah Keivan, Ganji Davood Domairry, . Optimization of conjugate heat transfer in the electrofusion joint using Taguchi method. Thermal Science. 2019; 23(5): 10.

[14] Jamshidi N, Farhadi M, Ganji DD, Sedighi K. Experimental analysis of heat transfer enhancement in shell and helical tube heat exchangers. Applied Thermal Engineering. 2013; 51(1): 644-52.

[15] Jamshidi N, Farhadi M, Sedighi K, Ganji DD. Optimization of design parameters for nanofluids flowing inside helical coils. International Communications in Heat and Mass Transfer. 2012; 39(2): 311-7.

[16] Jamshidi N, Mosaffa A. Investigating the effects of geometric parameters on finned conical helical geothermal heat exchanger and its energy extraction capability. Geothermics. 2018; 76: 177-89.

[17] Bayareh M, Mohammadi M. Multi-objective optimization of a triple shaft gas compressor station using Imperialist Competitive Algorithm. Applied Thermal Engineering. 2016; 109: 384-400.

[18] Lv H, Chen, Xueye, Zeng, Xiangwei. Optimization of micromixer with Cantor fractal baffle based on simulated annealing algorithm. Chaos, Solitons & Fractals. 2021; 148(C).

[19] Lv H, Chen X, Wang X, Zeng X, Ma Y. A novel study on a micromixer with Cantor fractal obstacle through grey relational analysis. International Journal of Heat and Mass Transfer. 2022; 183: 122159.

[20] Biçer N, Engin T, Yaşar H, Büyükkaya E, Aydın A, Topuz A. Design optimization of a shell-and-tube heat exchanger with novel three-zonal baffle by using CFD and taguchi method. International Journal of Thermal Sciences. 2020; 155: 106417.

[21] Thondiyil D, Kizhakke Kodakkattu S. Optimization of a shell and tube heat exchanger with staggered baffles using Taguchi method. Materials Today: Proceedings. 2021; 46: 9983-8.

[22] Hashimoto H, Ochiai M. Optimization of groove geometry for thrust air bearing to maximize bearing stiffness. Journal of Tribology. 2008; 130(3): 031101.

[23] Li X, Wang K, Du B. The Structure Optimization of T-slots Dry Gas Seal Faces. International Conference on Advanced Material Science and Environmental Engineering. 2016.

[24] Su H, Rahmani R, Rahnejat H. Thermohydrodynamics of bidirectional groove dry gas seals with slip flow. International Journal of Thermal Sciences. 2016; 110: 270-84.

[25] su H, Rahmani R, Rahnejat H. Performance Evaluation of Bidirectional Dry Gas Seals with Special Groove Geometry. Tribology Transactions. 2016; 60: 58-69.